Proceedings of the 27th International Symposium on Power Semiconductor Devices & IC's
May 10-14, 2015, Kowloon Shangri-La, Hong Kong

Simulation studies for Avalanche induced short-circuit current crowding of MOSFET-Mode IGBT

Masahiro Tanaka
Nihon Synopsys G.K.
2-21-1 Tamagawa, Setagaya-ku, Tokyo, 158-0094, JAPAN.
E-mail: mtanaka@synopsys.com

Akio Nakagawa
Nakagawa Consulting Office, LLC.
3-8-74 Hamatake, Chigasaki-city, Kanagawa, 253-0021, JAPAN.
E-mail: akio.nakagawa@nifty.com

***Abstract*—In this paper, new theory of device failure for MOSFET-Mode IGBTs is presented, for the first time, based on large scale 3D & 2D TCAD simulations. It was found that current filaments appear when the impact ionization in the anode side exceeds a critical avalanche generation rate. The current filamentation occurs because there exist two solutions: state of current filaments and state of uniform current flow beyond the critical avalanche generation rate. Below the critical avalanche rate, there is no state of current filaments, and the device is safe. The calculated results successfully explain the previous experimental results of device failure.**

I. INTRODUCTION

The short circuit withstand capability is still an essential topic in IGBT development. In the proceedings of ISPSD'14[1], we presented that the current filaments were observed in MOSFET-Mode IGBTs[2] during the short-circuit operation in spite of homogeneous channel electron current flow and completely symmetric cell structures. The degradation of the SOA of MOSFET-Mode IGBTs was theoretically attributed to the large impact ionization in the anode side, for the first time, in Ref.[3]. In Refs.[4, 5], the trigger of the current filament formation was tried to be explained by a positive feedback associated with the potential distribution and the saturated carrier drift velocities. However, the current filament formation mechanism has not been completely clarified yet.

MOSFET-Mode IGBT is defined in such a way that the anode efficiency $\gamma(=J_p/J)$ is less than γ_{MOS}, which represents $\mu_p/(\mu_p+\mu_n)$. γ and γ_{MOS} are defined at the N-base N-buffer junction. The γ_{MOS} value dynamically changes as the electric field or the lattice temperature changes inside the device because the mobility μ_p and μ_n are functions of the electric field and the lattice temperature.

The net charge ρ in the high field region can be calculated with the donor density N_D.

$$\rho = N_D + p - n = N_D + \left(\frac{\gamma}{v_h} + \frac{\gamma-1}{v_e}\right)\frac{J}{q}$$

$$= N_D + \left(\frac{v_h+v_e}{v_h v_e}\right)(\gamma-\gamma_{MOS})\frac{J}{q} \quad (1)$$

$$\gamma_{MOS} = \frac{\mu_p}{\mu_p+\mu_n} = \frac{v_h}{v_h+v_e} \quad (2)$$

where v_e and v_h are saturation velocities. For the high electric field case, γ_{MOS} is given by Eq.(2). When the anode efficiency γ is less than γ_{MOS}, the second term in Eq.(1) is negative, and the net charge ρ becomes negative for sufficiently large current density J. Once the net charge becomes negative, the peak high electric field region appears in the anode side of the N-base as shown in Fig. 1.

In this paper, we present a new theory of device destruction for MOSFET-Mode IGBTs, based on large scale 3D & 2D TCAD simulations. First, we show the calculation results, which explain the previous experimental results of device failure. Then, we discuss about the critical avalanche generation rate, which gives the criteria if the current filament occurs or not.

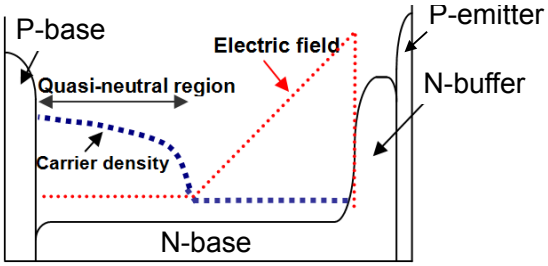

Fig. 1. Electric field distribution during short-circuit operation of MOSFET-mode IGBT. High electric field region appears in the anode side for high current density cases.

II. TCAD SIMULATION SETUP

Short circuit TCAD simulations with large scale 3D & 2D IGBT structure were performed. TCAD Sentaurus Device was used for all the simulations.

First, short circuit simulations for the 3D IGBT structure were performed to observe the lattice temperature rise due to the current filament formation and to estimate the time lag to device failure. The analyzed 3D structure had 8 identical IGBT cells 160um in width and 80um in depth as shown in Fig.2.

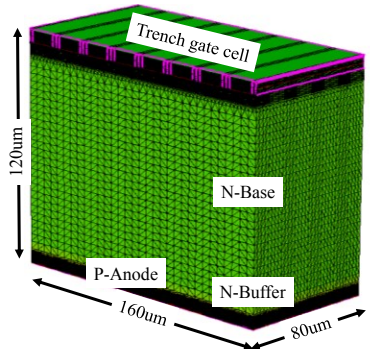

Fig. 2. 3D IGBT structure to estimate the time lag between current filament formation and device destruction. It has 8 IGBT cells, whose dimensions are 160um in width, 80um in depth and 120um in thickness. The number of the mesh points is approximately 870,000.

Then, short circuit simulations for the 2D structure of 320um wide 16 identical IGBT cells were performed for the applied DC voltages (V_{CC}), ranging from 200V to 1000V. The simulated IGBTs were 1.2kV rated and had the N-base

thickness of 120um. The doping concentrations of the P-emitter and the N-buffer were set such that the injection efficiency was less than 0.27 at the rated current density to realize MOSFET-Mode operation. The structures had completely uniform identical multiple cells and meshes. Self-heating was taken into account except Figs. 12 and 13. The thermal resistance of 0.3K/W was set between the anode electrode and the heat-sink. The heat-sink temperature was 300K. The simulation included lattice temperature dependence, high field saturation and carrier-carrier scattering as well as the University of Bologna avalanche model.

III. Results and Discussion

A. 3D Simulation Results

It was shown that the three-dimensional 8-cell structure showed quicker lattice temperature increase during the short-circuit operation than 16-cell 2D structure, as seen in Fig.3. The maximum lattice temperature exceeded the melting point of Silicon 1.4us after current filaments appeared. It can be assumed from the 3D simulation result that in the short-circuit operation, the device fails in approximately 1.5us once the current filaments are formed.

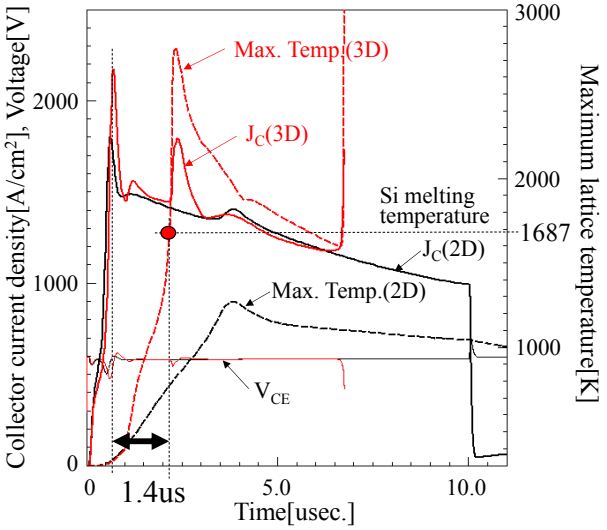

Fig. 3. Comparison of the short-circuit waveforms and the maximum lattice temperature changes between 3D and 2D IGBT simulations. In the 3D case, the maximum lattice temperature exceeds the melting point of Silicon after 1.4us from current filament formation.

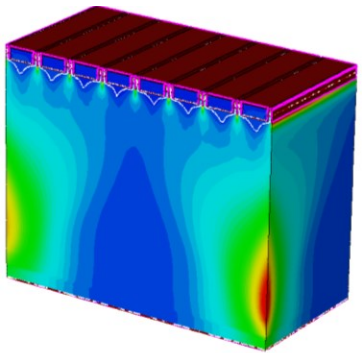

Fig. 4. Electron current density distribution of the 3D structure for t=2.0us. The current filaments appear on the edges of the structure.

B. 2D Simulations for Current Filament Formation

In Fig. 5, the critical current density for the current filament formation is shown as a function of DC voltage when 2D simulations of 3us short-circuit are performed. The current filaments are universally observed even for the applied DC voltage (V_{CC}) as low as 200V or for 1000V as seen in Figs. 6 to 9. For lower DC voltage of 200V, a higher current density is required to create high electric field in the N-buffer N-base junction for the current filament formation. For higher DC voltage (>700V), the filament formation is retarded because a high electric field is created throughout the N-base as seen in Fig. 10, suppressing laterally spreading electron current flow. Thus, more dense current filaments appear as seen in Fig. 9. The pitch of the current filaments is 107um, which is narrower than that of Fig. 7. The critical current density to form the current filaments takes a minimum value around the DC voltages of 400V to 700V as shown in Fig. 5. From the 3D simulation results, the critical current density can be regarded as the device destruction current density. Thus, Fig. 5 also shows the theoretical destruction current density as a function of the DC voltage, and well interprets the experimental results of Ref.[5], which is plotted also in Fig. 5.

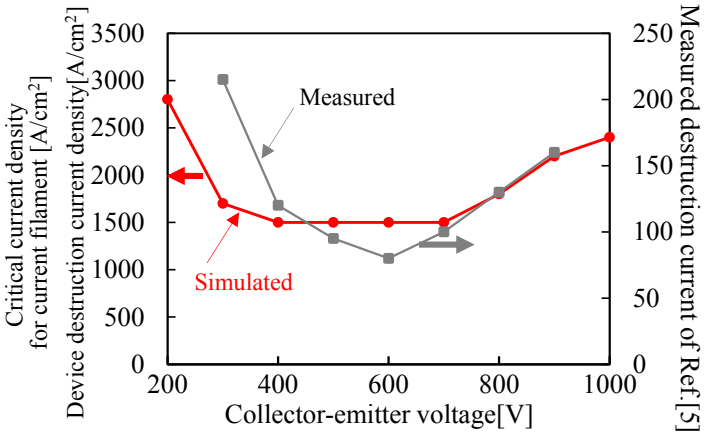

Fig. 5. Critical current density (red line) for the current filaments formation are plotted as a function of the collector-emitter voltage, when 2D simulations of 3us short-circuit are performed. From 3D results, the critical current density for the current filaments formation can be regarded as the device destruction current density. The simulated results agree well with the experimental results of Ref.[5].

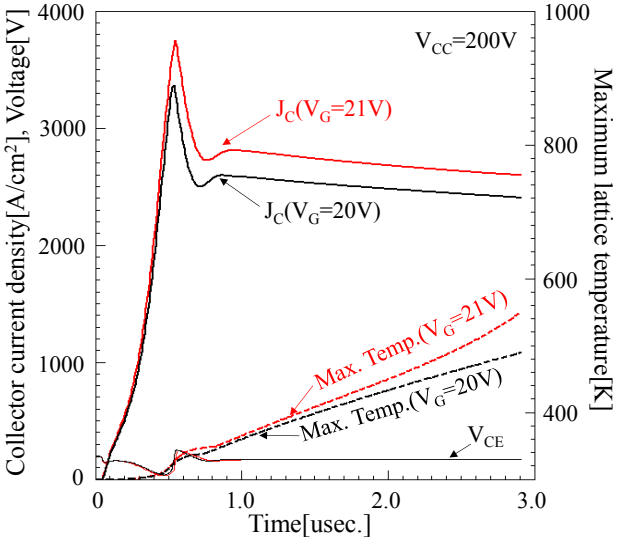

Fig. 6. 2D simulation results of the short-circuit waveforms for V_{CC}=200V. The current filaments appear when V_G is equal to or greater than 21V.

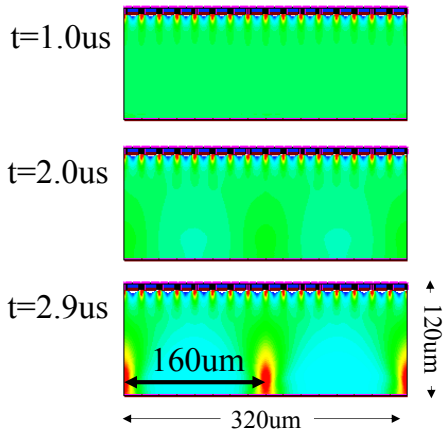

Fig. 7. Electron current density distribution of the 2D structure for t=1.0us, 2.0us and 2.9us when V_G=21V and V_{CC}=200V. The current filaments appear at t=2.0us. The pitch of the current filaments is 160um.

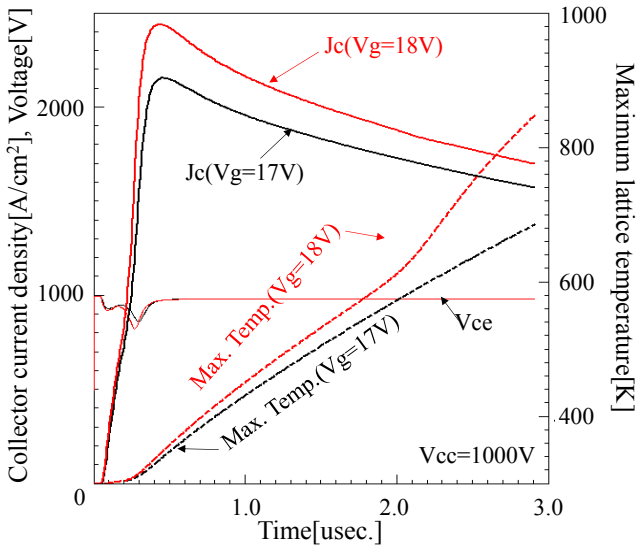

Fig. 8. 2D simulation results of the short-circuit waveforms for V_{CC}=1000V. The current filaments appear when V_G is equal to or greater than 18V.

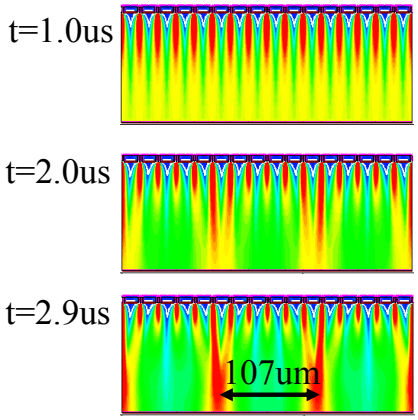

Fig. 9. Electron current density distribution of the 2D structure for t=1.0us, 2.0us and 2.9us when V_G=18V and V_{CC}=1000V. The current filaments appear at t=2.0us. The pitch of the current filaments is 107um. It is narrower than Fig.7 due to higher electric field throughout the N-base.

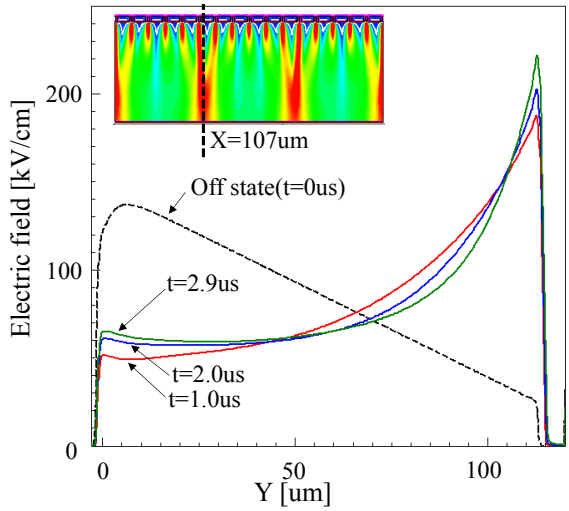

Fig. 10. Electric field distributions for the cross section of X=107um for t=0, 1.0, 2.0, and 2.9us, corresponding to Fig.9. The magnitude of the electric field is large throughout the N-base. Still, the magnitude of the electric field at the anode-side increases as the collector current density increases. The current filaments appear, when the avalanche generation rate becomes sufficiently large.

C. Theory for Current Filament

The critical avalanche generation rate, when the current filament appears, is plotted as a function of the applied DC-voltage in Fig.11. All the simulations in this section were executed in the isothermal condition in order to simplify the phenomena and to present readers a clear picture of current filamentation. If we take into consideration the self-heating, the critical avalanche generation rate depends on the lattice temperature, and differs considerably if the lattice temperature increases. However, it should be noted that the observed critical avalanche rate did not change considerably even when the self-heating is included because the lattice temperature rise at this moment is low.

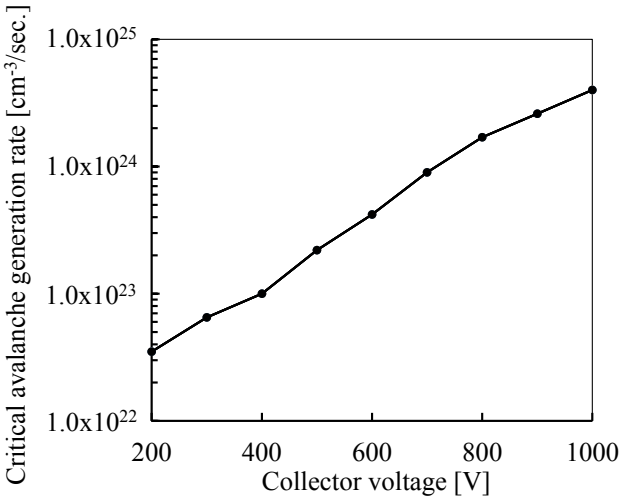

Fig. 11. The critical avalanche generation rate when the current filaments appear is plotted as a function of applied DC voltage.

It was confirmed that the current filaments appear when the devices are turned-on in the short-circuit mode and the avalanche generation rate exceeds the critical value. Fig.12 shows the locus of the collector current density vs. the maximum avalanche generation rate observed inside the device in the short-circuit operation, together with the static solutions for 600V DC voltage.

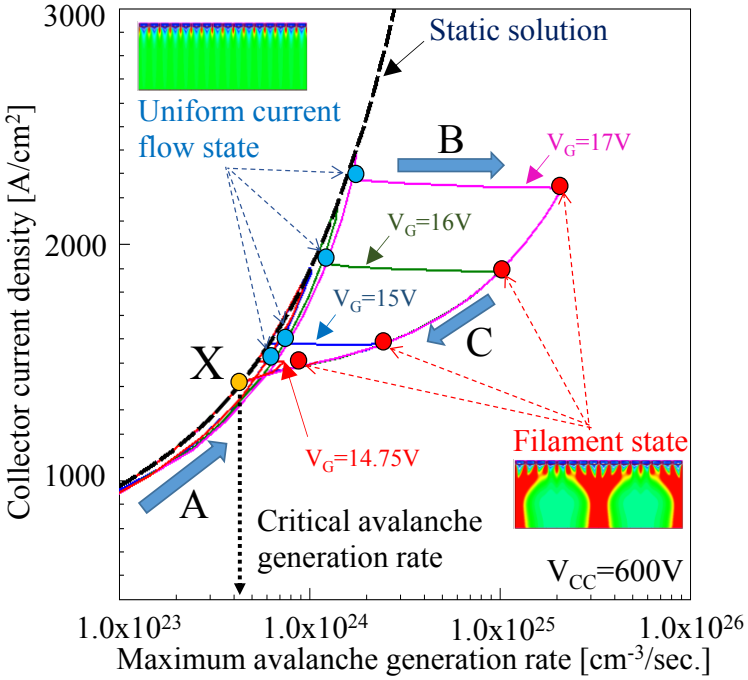

Fig. 12. Locus curves of the collector current vs. the maximum avalanche generation rate are plotted for the short-circuit waveforms when V_{CC}=600V and V_G=14.75V, 15V, 16V, 17V. When V_G>14.75V, large avalanche generation occurs and the locus moves to the state of filaments.

In Fig. 12, the locus of the static solution (dashed line) shows the state of uniform current flow. In the beginning of the short-circuit operation, the locus of the short-circuit operation closely traces the locus of the static solution (Arrow A of Fig.12). When V_G is greater than 14.75V, large avalanche generation, exceeding the avalanche rate of uniform current flow, occurs and the system moves to the state of current filaments from a transient state of uniform current flow (Arrow B). After current filaments have appeared, the system stays in a state of current filament in the isothermal simulation. Then, if we slowly decrease V_G, the system returns to the state of uniform current flow, tracing the locus along the Arrow C in the figure. The locus along the Arrow C goes through all the states of current filaments of V_G>14.75V. For V_G>14.75V, the system commonly traces the locus along the Arrow C, if we decrease V_G after the current filamentation has occurred. Eventually, the locus of the states of current filaments joins to the state of uniform current flow at the critical avalanche generation rate (yellow point X) as shown in Fig. 11. It should be noted that the return to the state of uniform current flow from the states of current filaments occurs only in isothermal simulations. If we switch on the self-heating, the device burns out instantly, once current filaments are formed.

There coexist the state of uniform current flow and the states of current filaments beyond the critical avalanche rate. The current filament appears automatically if the magnitude of the avalanche generation becomes large and exceeds the critical value in the short-circuit operation just because the states of current filaments exist beyond the critical avalanche generation rate.

The states of current filaments can be reproduced not only in the transient short-circuit simulations but also in static simulations. Fig. 13 shows J_C(max)-V_G curves, calculated by static simulation of I_C-V_G characteristics with changing the numerical conditions such as the voltage sweeping steps or the convergence accuracy. The black line corresponds to a state of uniform current flow, and the red dashed line and blue dotted line show two states of current filaments, respectively. It means that a state of uniform current flow is not quite stable. The red dashed line, starting from V_G=15V, traces the locus similar to the filament state of Fig. 12. However, the appearance of the current filament is different from Fig. 12. It is suggested that a state of current filament is not uniquely determined for a collector or a gate voltage.

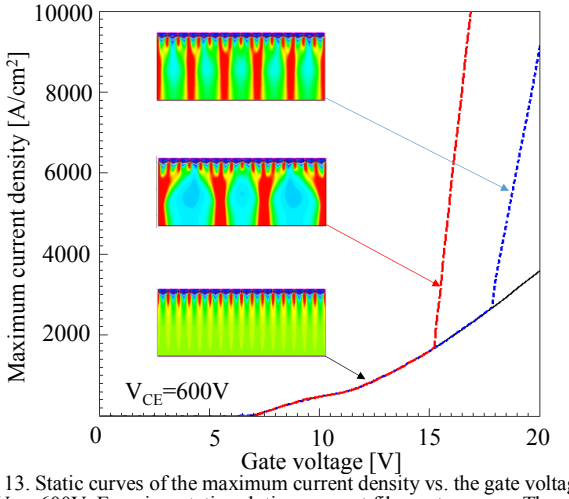

Fig. 13. Static curves of the maximum current density vs. the gate voltage for V_{CE}=600V. Even in a static solution, current filaments appear. The red dashed line starting from V_G=15V, traces the locus similar to the filament state of Fig. 12. The appearance of the filaments is different from Fig. 12.

IV. Conclusion

New destruction theory of MOSFET-Mode IGBT is proposed. We present three important results. First, devices fail in approximately 1.5us once current filaments form. Second, it was found that the current filaments appear because there exist the states of current filaments when the avalanche generation rate exceeds the critical value, which is shown in Fig.11. Beyond the critical avalanche rate, there coexist two kinds of states: a state of uniform current flow and states of current filaments. Below the critical rate, there is no state of current filament, and the device is safe. Third, the current filamentation is considered to be the main origin of the device failure. The simulated results successfully explain the previous experimental data of Ref.[5].

References

[1] M. Tanaka and A. Nakagawa, "Simulation studies for short-circuit current crowding of MOSFET-Mode IGBT", Proc. of ISPSD'14, pp.119-122, 2014.

[2] T. Matsudai and A. Nakagawa, "Ultra high switching speed 600V thin wafer PT-IGBT based on new turn-off mechanism", Proc. of ISPSD'02, pp.285-208, 2002.

[3] A. Nakagawa, T. Matsudai, T. Matsuda, M. Yamaguchi and T. Ogura, "MOSFET-mode Ultra-Thin Wafer PTIGBTs for Soft Switching Application - Theory and Experiments" Proc. of ISPSD'04, pp.103-106, 2004.

[4] A. Kopta, M. Rahimo, U. Schlapbach, N. Kaminski and D. Silber, "Limitation of the short-circuit ruggedness of high-voltage IGBTs", Proc. of ISPSD'09, pp.33-36, 2009.

[5] R. Baburske, V. Treek, F. Pfirsch, F.-J. Niedernostheide, C. Jaeger, H.-J. Schulze and H. P. Felsl, "Comparison of Critical Current Filaments in IGBT Short Circuit and during Diode Turn-off", Proc. of ISPSD'14, pp.47-50, 2014.